Acta Pathol. Jpn.
30(4): 515~530, 1980

IMMUNOPATHOLOGY OF RHINO MOUSE, AN AUTOSOMAL RECESSIVE MUTANT WITH MURINE LUPUS-LIKE DISEASE

Hisanori KAWAJI, Ryoichi TSUKUDA, and Takeshi NAKAGUCHI

Biological Research Laboratories, Central Research Division, Takeda Chemical Industries Ltd., Osaka

(Received on July 24, 1979)

Detection of high incidence of antinuclear antibodies (ANA) was reported in young homozygous rhino mice employing formalinized chicken erythrocyte nuclei as substrate for indirect immunofluorescence (IF) assay. The titers of ANA heightened with increasing age, and attained to 1:1024 by the time mice reached 5 months of age. The occurrence of ANA was associated with development of splenic and hepatic fibrosis, glomerulonephritis and abnormalities of lymphoreticular tissue. The granular deposits of IgG and C3 detected by direct IF were initially found at the basement membrane of dermal-epidermal junction of rhino mice aged 2.5 months. These deposits distributed progressively in the fibrotic areas of spleen and liver, and renal glomerular tufts at 5 months of age. Dense deposits revealed by electron microscopy were found in the regions where IF of IgG and C3 was observed. Acid buffer eluates from liver and kidney contained IgG reactive with nuclear antigens. Importance of homozygous rhino gene was discussed in relation to development of autoimmune disorders of these mice. ACTA PATHOL. JPN. 30: 515~530, 1980.

Introduction

The rhino mouse, reported by HOWARD[12] for the first time, is a mutant having abnormal integument which is characterized by rhinoceros-like, hairless and wrinkled skin[5,12]. The character is governed by the autosomal recessive gene hr^{rh} which is an allele of hairless gene and is located in linkage group III[12]. The present authors[15,16] have described the morphological and functional abnormalities of antibody forming organs of this mouse together with spontaneous hypergammaglobulinemia, implicating that the mouse has perhaps a systemic disease of autoimmune nature in addition to the phenotypic skin abnormalities.

The roles of the genetic factors influencing immune responses and development of autoimmune disorders have been repeatedly emphasized in the recent literature of immunology[19,32]. The spontaneous disease of New Zealand mice has been found to be a unique model for human autoimmune diseases, such as systemic lupus erythematosus and autoimmune hemolytic anemia[6,11,18,23,26,32]. Genetic studies have been extensively

川路 尚徳, 佃 良一, 中口 武
Mailing address: Hisanori KAWAJI, Biological Research Laboratories, Central Research Division, Takeda Chemical Industries, Ltd., Yodogawa-ku Jusohonmachi 2-17-85, Osaka 532, JAPAN.

performed with New Zealand mice in many laboratories and the development of autoimmune diseases seems to be controlled by multiple autosomal genes[32].

More recently, congenitally athymic nude mice, which are autosomal recessive mutants, also developed early manifestations of spontaneous autoimmunization, as shown by the presence of circulating antinuclear antibodies (ANA) and immunoglobulin deposits in the glomeruli of the kidney[16,27].

In the present paper, we reported the results of studies on the immunopathological abnormalities of rhino mice at various ages. The significance of deposition of immune complex is shown in relation to the development of systemic chronic lesions and the genetic background of these mice.

Materials and Methods

Mice: The present stock of rhino mice (Fig. 1) with BALB/c background was first introduced from Zoological Laboratories of Hokkaido University in 1963. In 1967, specific pathogen free (SPF) colonies were obtained by Caesarian operation followed by foster nursing with SPF ICR mice in a vinyl isolator in our laboratory. Thereafter, they were maintained in the barrier sustained system at 23±2°C, and 55±5% humidity. The repeated microbiological examinations have proved that the environment was free from following microorganisms: Sendai virus (HVJ), mouse hepatitis virus (MHV), Mycoplasmas, Tyzzer, Corynebacteriae, Salmonellae, other common pathogenic bacteriae. Details of genetic background, care and maintenance of rhino mice have been previously described[15,16].

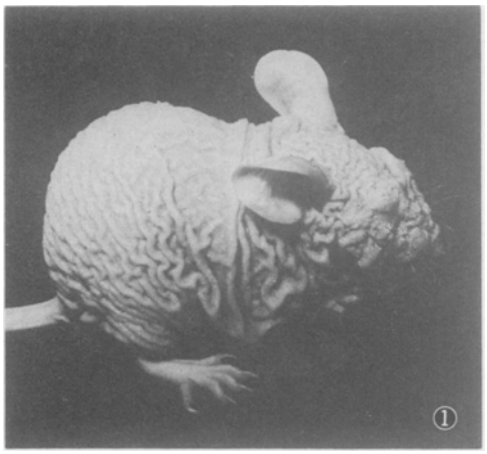

Fig. 1. Photograph of an adult rhino mouse showing characteristic hairless and wrinkled skin. Remaining vibrissae and elongated nails are noted.

Four to 25-week-old SPF DBA, C3H, C57BL/6, and ICR mice were obtained from colonies maintained at Drug Safety Research Laboratories, Central Research Division, Takeda Chemical Industries, Ltd..

Conventional and SPF colonies of nude mice were delivered from Dr. K. Suzuki (The Institute of Medical Sciences, The University of Tokyo) and Dr. T. Nomura (Central Institute for Experimental Animals), respectively. These mice were maintained in vinyl isolators and were given sterilized food (CE-2, Japan CLEA, Inc.) and water *ad libitum*.

Sera: The blood was collected with sterilized hematocrit capillary tubes from the orbital venous plexus of each mouse. Centrifugation was carried out for 5 minutes in a micro-hematocrit centrifuge (Marusan-Superior, Sakura Seisakusho Ltd., Tokyo). The tubes were then broken above the clot and the sera were collected in the sterilized micro-sample tubes, then stored at -20°C until use.

Detection and titration of ANAs: ANAs in the sera were detected by the usual indirect IF method. Chicken erythrocyte nuclei were commonly used as nuclear substrate for screening test of incidence of ANA. After air-drying, smears of chicken erythrocytes were fixed in 95% ethanol at 4°C for 10 minutes and stored at 4°C until subsequent test. The smears of substrate were covered with one drop of test serum and incubated at 37°C for 30 minutes in moisture chambers. After washing in 0.01 M PBS, pH 7.1, rabbit anti-mouse IgG antibody conjugated with FITG was applied at 37°C for 30 minutes, then the slides were washed with PBS and mounted in buffered glycerol. The slides were examined under a Zeiss fluorescent microscope equipped with Osrum HBO 100/2 lamp utilizing Ploem's vertical illumination with an exciter filter BG–12, beam splitter FL–500 and barrier filter 50. Although titers of ANAs were similarly determined by indirect IF method after diluting the sera up to 1:1024 in the microtiter plates, formalinized chicken erythrocyte nuclei[33] were used as substrate in order to elevate the sensitivity. Other substrates, such as rat Yoshida sarcoma cells, cultured rabbit kidney cells and gold fish erythrocytes were also used in some experiments.

Light microscopy: Tissues of mice were fixed in 10% neutral formalin or Carnoy's solution, embedded in paraffin, cut into 4 μ sections and routinely stained by hematoxylin and eosin. Special stains employed were: May-Grünwald-Giemsa, PAS, Masson trichrome, methyl green-pyronin, alcian blue-chronantin fast red and Gomori's silver impregnation.

Electron microscopy: Small pieces of cutaneous, hepatic and renal tissues were fixed in 2.5% glutaraldehyde in 0.1 M phosphate buffer, pH 7.2 and then 1% osmium tetroxide. They were embedded in Epon 812 and cut on a LKB ultramicrotome. The sections were stained with uranyl acetate and lead citrate and examined with a JEM-100B electron microscope.

Detection of tissue-bound immunoglobulins and complement:

Rabbit anti-mouse IgG, IgM and C3 conjugated with FITC were purchased from Miles Laboratories. Tissues used for detection of IgG and IgM were fixed in 95% ethanol at 4°C, dehydrated and embedded in soft paraffin according to Sante-Marie's method[28]. Deparaffinized sections were stained by the direct IF method for IgG or IgM. Cryostat sections, fixed with cold 95% ethanol, were used for detection of C3. Control sections were incubated with unfluorescinated rabbit anti-mouse IgG, IgM or C3 antibodies prior to incubation with FITC labeled antibodies.

Elution of tissue-fixed globulin: Elution procedures were performed as described by Lambert and Dixon[18] with certain modifications. Briefly, tissues of liver, kidney, spleen, lymph node and skin were minced in PBS and washed five times by decanting to remove blood. The mince was homogenized in a Waring Blender at 4°C. The suspension was centrifuged and washed five times with 30 vol. of PBS. The supernatant was concentrated with Centriflo, CF25 (Amicon, Far East) and examined for the presence or absence of ANA. The washed tissue sediment was suspended in 0.02 M citrate buffer pH 3.2, and incubated at 37°C for 90 minutes. As control, one part of tissue was incubated with citrate buffer pH 7.2. After centrifugation, an equal volume of saturated ammonium sulfate was added to the supernatant. The precipitate formed was dissolved in PBS, dialyzed extensively against PBS, concentrated with Centriflo, CF25 and tested for ANA by indirect IF. The eluates were also analyzed by immunoelectrophoretic[34] and radial immunodiffusion methods[21].

Results

Detection of ANA by IF Method

Indirect IF method utilizing ethanol-fixed nucleated cells as substrate demonstrated that ANA was present with high incidence in the sera of rhino mice. An example of IF of chicken erythrocyte nuclei is depicted in Fig. 2. DNase treatment before staining abolished or markedly decreased nuclear IF of chicken erythrocyte nuclei, while RNase treatment did not affect nuclear staining. Results of the survey for ANA activity in undiluted sera of rhino mice are shown in Figs. 3 and 4. The numbers of ANA positive animals increased with aging. Incidence of ANA in hr^{rh}/hr^{rh} mice was 86% (31 out of 36) at 5–7 months and 99% (74 out of 75) over 7 months of

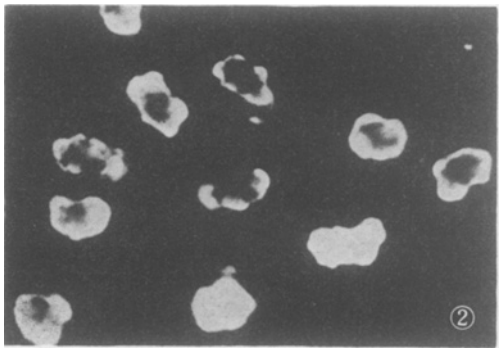

Fig. 2. IF of chicken erythrocyte nuclei showing peripheral staining pattern. Indirect IF Method. × 840.

age. On the other hand, the incidence of ANA in haired littermates was low, but increased gradually with aging. Haired $hr^{rh}/+$mice were intermediate in incidence of ANA between hr^{rh}/hr^{rh} mice and haired littermates.

Incidence of ANA in control mice, such as C3H, DBA, C57BL/6, ICR and nude mice was also surveyed by IF technique and only homozygous nude mice (nu/nu) developed frequently ANA.

Serum titers of ANA in hr^{rh}/hr^{rh}, $hr^{rh}/+$ and other strains of mice are shown in Fig. 5. A remarkable elevation of ANA titer was found in male and female

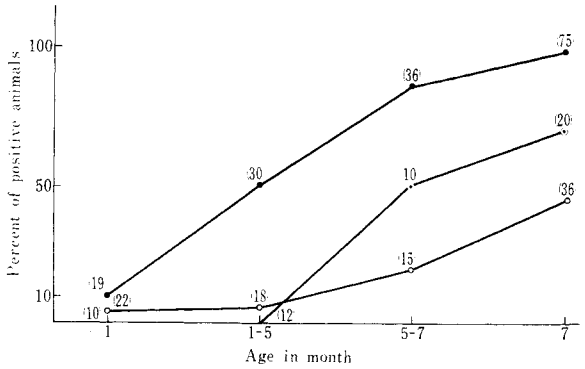

Fig. 3. Incidence of ANA in rhino mouse. ●: hr^{rh}/hr^{rh} (mice homozygous for rhino gene), ◉: $hr^{rh}/+$ (mice heterozygous for rhino gene), ○: haired littermate (mice not determined for presence or absence of heterozygous rhino gene). Numerals in parentheses indicate numbers of animal tested.

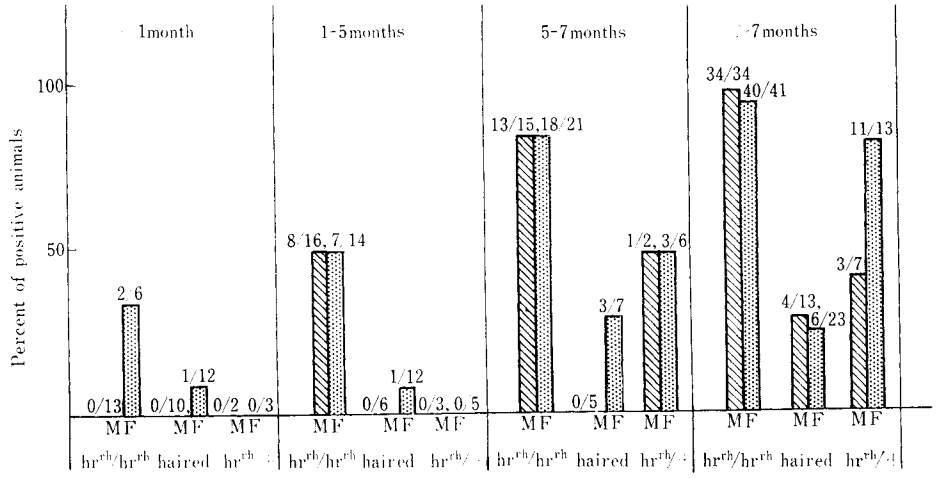

Fig. 4. Incidence of ANA in male and female rhino mice at various ages. M: Male, F: Female Numerator: No. of mice with ANA, Denominator: No. of mice tested. hr^{rh}/hr^{rh}: Mice homozygous for rhino gene, $hr^{rh}/+$: Mice heterozygous for rhino gene, haired: Haired littermate (mice not determined for presence or absence of heterozygous rhino gene).

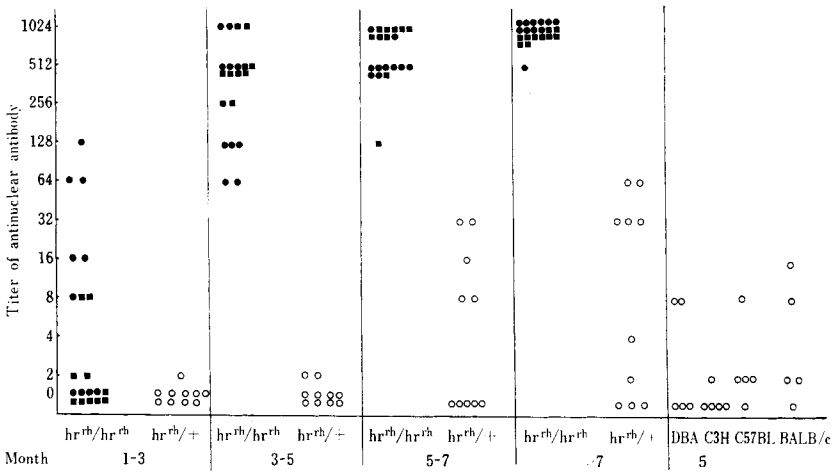

Fig. 5. Serum titers of ANA in rhino mice using isolated chicken erythrocyte nuclei as substrate. ■: male hr^{rh}/hr^{rh} mice, ●: female hr^{rh}/hr^{rh} mcie, ○: female haired mice.

hr^{rh}/hr^{rh} mice with increasing age. Over 7 months of age 20 out of 21 showed positive IF of ANA in 1:1024 serum dilution and only one showed 1:512. In contrast to the high titer observed in hr^{rh}/hr^{rh} mice, ANA reactions of $hr^{rh}/+$ mice and other strains, such as DBA, C3H, C57BL/6 and BALB/c mice were generally negative at a younger age, but only slight elevations of ANA titer were found at advanced age.

Histopathologic and Immunopathologic Findings

Age-related histopathological changes in 92 (32 males and 60 females) hr^{rh}/hr^{rh} mice and 58 (19 males and 39 females) haired littermates including $hr^{rh}/+$mice are summarized in **Table 1**. Because no quantitative sex difference was found in the lesions, the changes in both sexes were indiscriminatingly tabulated in this **Table**. A variety of severe lesions was noted in hr^{rh}/hr^{rh} mice, but only small numbers of lesions with minimal severity were found in haired littermates.

Time-sequence of IgG localization in various organs of several hr^{rh}/hr^{rh} and $hr^{rh}/+$ female mice as detected by direct IF is shown in **Table 2**. Localization of IgG in plasma cells of spleen and lymph node and in the skin were detectable as early as 2.5 months of age in hr^{rh}/hr^{rh} mice and by 5 months the IgG depositions were found in the fibrotic areas of liver, renal glomerulus, and in the cornea and sclera of eye of hr^{rh}/hr^{rh} mice. These changes were not found in $hr^{rh}/+$ mice examined.

Details of histopathological and IF findings in the individual organs of hr^{rh}/hr^{rh} mice during aging are as follows:

Thymus: The thymus showed normal structure in mice younger than 2 months of age. The cortico-medullary border was clear and small lymphocytes in the cortex were abundantly found at this stage. Slight thymic atrophy with a decrease in cortical small lymphocytes was observed between 3 to 5 months of age. The narrowing of the cortex accompanied by reduced staining activity was conspicuous after 6 months of age. The number of plasma cells containing IgG in the cytoplasm detected by IF

Table 1. *Summary of Histopathological Findings in Homozygous Rhino Mice and Haired Littermates*

Age in months		<2		2–4		4–6		6–11		>11	
		hr^{rh}/hr^{rh}	HL	hr^{rh}/hr^{rh}	HL	hr^{rh}/hr^{rh}	HL	hr^{rh}/hr^{rh}	HL	hr^{rh}/hr^{rh}	HL
		♯	*								
Thymus	Cortical atrophy	0/6	0/6	5/10	0/12	9/12	0/11	30/31	11/16	33/33	9/13
	Plasma cell infiltration	0/6	0/6	0/10	0/12	3/12	0/11	18/31	0/16	19/33	0/13
	Appearance of giant cell	0/6	0/6	0/10	0/12	0/12	0/11	11/31	0/16	17/33	0/13
Spleen	Depletion of lymphocyte in TDA	0/6	0/6	0/10	0/12	10/12	0/11	30/30	0/16	29/33	1/13
	Plasma cell hyperplasia	0/6	0/6	3/10	0/12	12/12	0/11	30/30	0/16	29/33	0/13
	Fibrosis	0/6	0/6	0/10	0/12	5/12	0/11	19/30	0/16	23/33	0/13
Lymph nodes	Decrease of lymphocyte from TDA	0/6	0/6	8/10	0/12	12/12	0/11	31/31	0/16	32/33	0/13
	Plasma cell hyperplasia	0/6	0/6	6/10	0/12	12/12	0/11	31/31	0/16	31/33	0/13
	Reticulum cell hyperplasia	0/6	0/6	6/10	0/12	12/12	0/11	30/31	0/16	32/33	0/13
	Appearance of giant cell	0/6	0/6	1/10	0/12	8/12	0/11	10/31	0/16	18/33	0/13
Liver	Appearance of various size of nuclei	0/6	0/6	1/10	1/12	9/12	1/11	27/31	4/16	32/33	7/13
	Fibrosis	0/6	0/6	0/10	0/12	10/11	0/11	20/31	0/16	29/33	0/13
	Plasma cell infiltration	0/6	0/6	0/10	0/12	9/11	0/11	23/31	0/16	29/33	0/13
	Eosinophil infiltration	0/6	0/6	2/10	1/12	9/11	1/11	20/31	2/16	29/33	0/13
Renal glomerulus	Increase in mesangial matrix	0/6	0/6	2/10	0/12	10/11	3/11	31/31	5/16	32/33	7/13
	Thickening of basement membrane	0/6	0/6	2/10	0/12	8/11	0/11	31/31	3/16	32/33	7/13
Skin	Cyst formation	6/6	0/6	10/10	0/12	11/11	0/11	30/30	0/16	32/32	0/13
	Cell infiltration in cutis	1/6	0/6	7/10	0/12	10/11	0/11	28/30	0/16	30/32	0/13

Severity of lesions was rated on an arbitrary scale of following grade: negative, minimal, moderate, severe, very severe.

♯: No. of homozygous rhino mice with lesions/No. of homozygous rhino mice examined.

*: No. of haired littermates with lesions / No. of haired littermates examined.

HL: Haired littermates.

TDA: Thymus dependent area.

Table 2. *Deposition of IgG in Various Organs of Homozygous Rhino Mice and Heterozygous Haired Littermates*

Age in month		1		2.5		5	
		hr^{rh}/hr^{rh}	$hr^{rh}/+$	hr^{rh}/hr^{rh}	$hr^{rh}/+$	hr^{rh}/hr^{rh}	$hr^{rh}/+$
Lymph node	Plasma cell in medullary cord	0/3°	0/3	5/9	0/9	6/6	0/6
Spleen	Plasma cell in red pulp	0/3	0/3	2/8	0/9	6/6	0/5
Liver	Area of fibrosis	—	—	—	—	5/5	—
Kidney	Glomerular mesangium	0/3	0/2	0/9	0/9	3/6	0/6
	Glomerular basement membrane	0/3	0/2	0/9	0/9	3/6	0/6
Skin	Basement membrane	0/3	0/3	6/9	0/9	6/6	0/6
	Connective tissue of dermis	0/3	0/3	6/9	0/9	6/6	0/6
Eye	Corneal stroma	0/3	0/2	0/6	0/6	5/5	0/5
	Sclera	0/3	0/2	0/6	0/6	5/5	0/5

°: No. of mice with plasma cells containing IgG or No. of mice with IgG deposition / No. of mice examined

method was increased in the thymus replacing the lymphocytes. Multinucleated giant cells were occasionally found in mice of advanced age. No germinal centers were seen in any of these thymuses.

Lymph node: No marked changes were observed in mice younger than 2 months of age. With advancing age, extensive development of germinal centers was found in the cortex and the number of small lymphocytes in the deep and midcortex, the so-called thymus-dependent areas, began to decrease in mice between 3 to 5 months of age. Decrease in the number of lymphocytes of these areas became more pronounced with advancing age, and these areas were mainly composed of plasma cells and reticulum cells. The plasma cell proliferation associated with Russell's body formation was markedly observed in the medullary cord. IF microscopy revealed the prominent localization of IgG in the cytoplasm of plasma cells. As the lesions progressed, the depletion of small lymphocytes and the appearance of bizarre giant cells were noted. Small numbers of lymphocytes remained in the sinus.

Spleen: No remarkable lesions were found in mice younger than 4 months of age. A depletion of lymphocytes around the central arteries of the white pulp, moderate reticulum cell hyperplasia and extramedullary hematopoiesis in the red pulp were found in mice between 4 to 6 months of age. Numerous plasma cells containing IgG were observed frequently in the red and white pulps. Splenic fibrosis, beginning around the central arteries of white pulp was frequently observed at about 5 months of age. In severe cases, the entire splenic parenchyma was gradually replaced with collagen fibers. Onionskin-like lesions were observed around the central arteries in mice older than 6 months of age. Concentrical deposition of IgG and C3 was detected at the site of periarterial fibrotic regions.

Skin: Hyperkeratosis and characteristic cyst formation accompanied by proliferation of subepithelial connective tissue were already observed at one month of age. A large amount of IgG was deposited in the subepidermal connective tissue chiefly along the collagen fibers of almost all the hr^{rh}/hr^{rh} mice at 2.5 months of age (Fig. 6). Characteristic bright fluorescence was detected along the basement membrane of dermal-epidermal junction (Fig. 7). Deposition of C3 were also detected by direct IF at the analogous regions, where IgG was deposited, but their staining patterns seemed to be more granular and lumpy than those of IgG.

Liver: Histopathological examination revealed that severe centrilobular and periportal fibrosis was consistently observed in the liver of hr^{rh}/hr^{rh} mice by 5 months of age (Fig. 8). The direct IF method showed extensive deposits of IgG (Fig. 9) and C3 in the sites of fibrosis of liver especially along the collagen fibers. Pronounced accumulation of plasma cells containing IgG in the cytoplasm was observed in the fibrous portions adjacent to the liver parenchyma (Fig. 9). Deposition of IgM was not detected in the fibrous portion of the liver.

Kidney: In the glomerulus of the kidney, thickening of the basement membrane, deposition of PAS positive materials (Fig. 10) and glomerulonephritis accompanied by the appearance of exudative lesions were frequently observed at 6 months of age. An adhesion of glomerular tuft to the Bowman's capsule (Fig. 10) and mesangial prolifera-

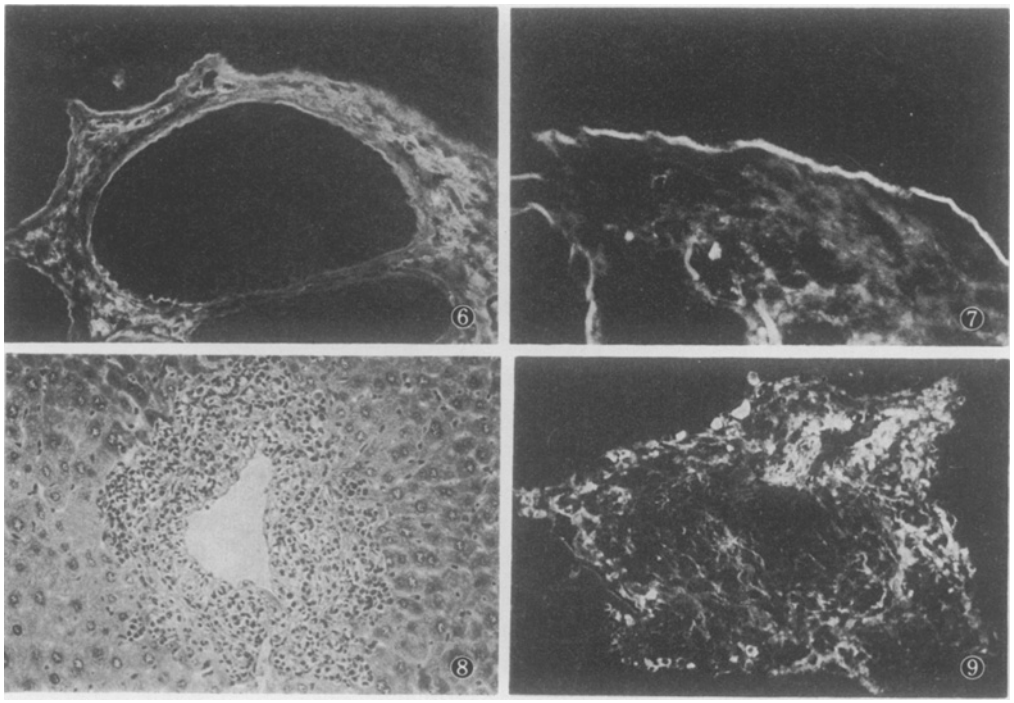

Fig. 6. Skin of rhino mouse showing conspicuous deposition of IgG in subepidermal connective tissue surrounding the cyst. Surface of the skin is at the upper corner of photo. Direct IF method. × 91.

Fig. 7. Higher magnification of skin of rhino mouse. IgG deposits are noted in the basement membrane of dermal-epidermal junction as well as in the subepidermal connective tissue. Direct IF method. × 370.

Fig. 8. Liver of rhino mouse showing severe fibrosis around a central vein. HE × 49.

Fig. 9. Liver of rhino mouse showing conspicuous deposition of IgG in region of fibrosis. Direct IF method. × 91.

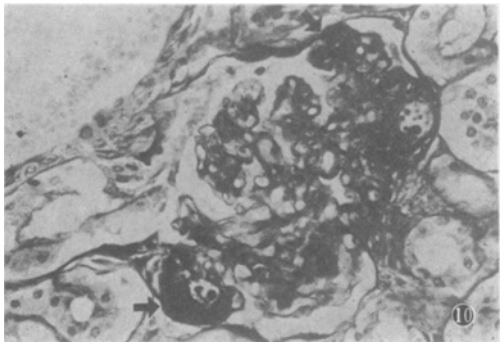

Fig. 10. Glomerulus of rhino mouse showing thickening of capillary basement membrane and marked deposition of PAS positive material. Adhesions of glomerular tuft to Bowman's capsule are also seen (arrows). PAS. × 190.

tion were also found by 6 months of age. IF studies revealed that lumpy and granular staining of IgG and C3 was distributed along the capillary basement membrane and in the mesangium of glomerulus (Figs. 11, 12). A small amount of IgM was also demonstrated along the basement membrane with lumpy and granular stain-

ing patterns. Periarterial infiltration of plasma cells containing IgG in the cytoplasm was occasionally observed in the kidney.

Eye: Eyes of rhino mice older than 6 months showed grossly corneal opacity. Histologically, long slender keratocytes, neovascularization, irregular arrangement of collagen fibers and neutrophil infiltration were noted in the corneal stroma. These changes progressed with advancing age. Deposition of IgG and C3 detected by IF was also found in the corneal stroma and sclera at 5 months of age.

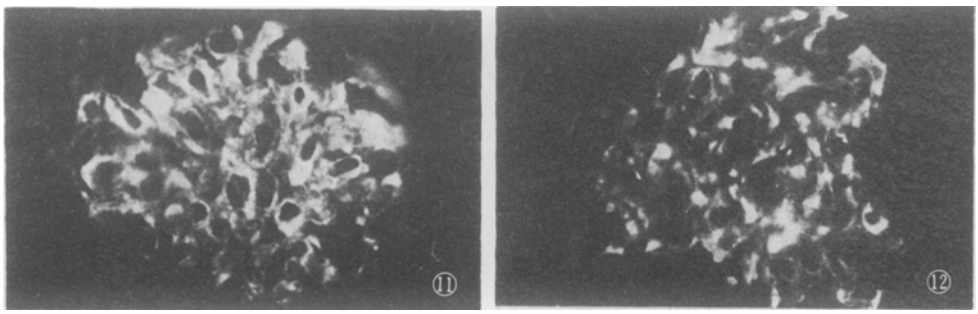

Fig. 11. Glomerulus of rhino mouse showing lumpy or granular deposition of IgG in the mesangium and along the capillary basement membrane. Direct IF method. × 210.
Fig. 12. Glomerulus of rhino mouse showing lumpy or granular deposits of C3 in the mesangium and along the capillary basement membrane. Direct IF method. × 210.

Electron Microscopy

Skins, livers and kidneys of rhino mice older than 6 months of age were studied by electron microscopy.

Skin: A slight thickening of basement membrane was found at the dermal-epidermal junction of skin. Many hemi-desmosomes connected with tonofilaments were found at the basal portion of basal epidermal cells. Collagen fibers intermingled with numerous microfibrils, presumably the fibrils of tropocollagen were located near the basement membrane. Electron-dense deposits were present at the dermal-epidermal junction or among collagen fibers. They appeared as dark, osmiophilic irregular areas with granular structure and occasionally attached to collagen fibers.

Liver: Fibrotic areas of liver were electron-microscopically observed. Numerous bundles of collagen fibers were located near the degenerated hepatic cells with vacuolated mitochondria. Electron-dense deposits with fine fibrillar structure were found among collagen fibers (Fig. 13). Accumulation of plasma cells was found among the collagen fibers especially adjacent to the hepatic parenchyma. Mature plasma cells with well-developed lamellar endoplasmic reticulum and immature ones with poorly-developed endoplasmic reticulum were found in these areas (Fig. 13).

Kidney: An irregular thickening of basement membrane associated with an enlargement of mesangial areas was generally found in the capillary loops of glomerulus (Fig. 14). A smooth, rounded projection towards the epithelial side, a so-called hump, was frequently found in the basement membrane. Epithelial cell foot processes were

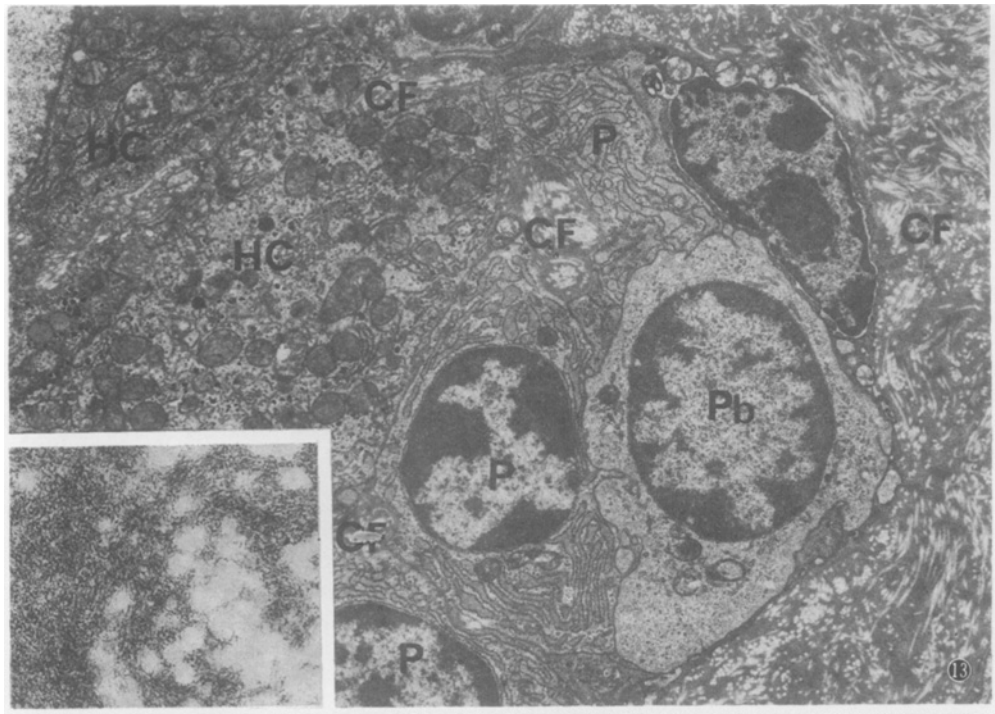
CF
HC
P
HC
CF
CF
Pb
P
CF
P
⑬

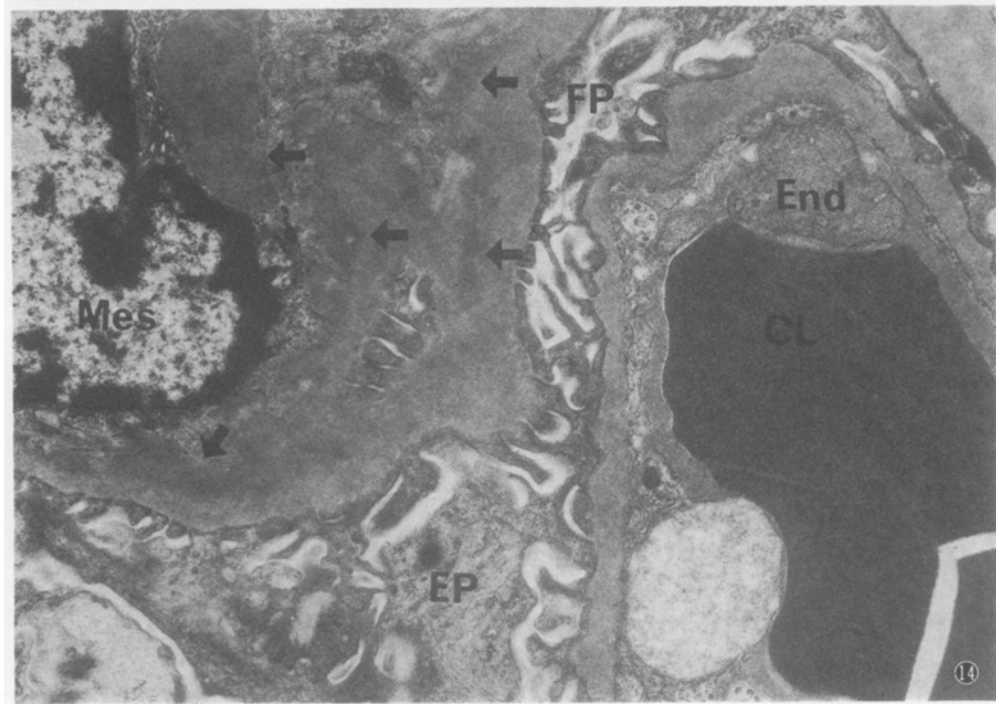
FP
End
Mes
CL
EP
⑭

often fused. Electron-dense deposits were located in the mesangial regions, within the basement membrane, between the basement membrane and epithelial cells, and between the basement membrane and endothelial cells. Among them, mesangial deposits were most frequently found (Fig. 14). These deposits showed amorphous or finely fibrillar structure. Cytoplasmic processes of mesangial cells were commonly seen near the dense deposits.

Characterization of Tissue Eluates

By an immunoelectrophoretic analysis, only IgG was detected in the acid buffer eluates (citrate buffer, pH 3.2) of livers and kidneys of rhino mice (Fig. 15). Detection of proteins other than IgG using anti-mouse serum was unsuccessful in the acid buffer eluates. Eluates from the livers and kidneys were found to have ANA reacting with chicken erythrocyte nuclei and their staining patterns were of a typical peripheral type. The concentrations of ANA activity in IgG eluted from livers and kidneys versus those of ANA activity in serum IgG was 2 to 4 times higher in eluates of livers and kidneys of hr^{rh}/hr^{rh} mice. Neither IgG nor ANA was detected in the concentrated PBS which was used for 3 times or more repeated washing of all the tissues examined, and in the neutral buffer eluates (citrate buffer, pH 7.2) of livers and kidneys. Acid and netural buffer eluates from spleens, lymph nodes and skins did not contain IgG nor ANA.

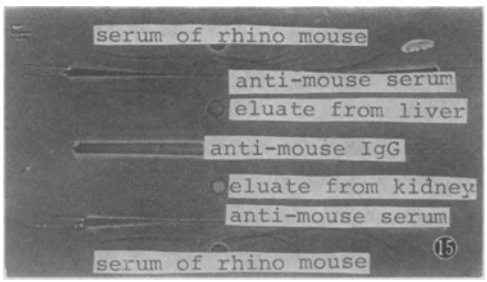

Fig. 15. Immunoelectrophoretic patterns of eluates from livers and kidneys of rhino mice. Both eluates contain IgG but no other serum protein.

Discussion

It has long been recognized that rhino mice are mutant mice having abnormal integument which is characterized by hairless and wrinkled skin. Although these mice have been extensively used as experimental tools in many fields of research, such as morphology, and phenotypic expression of skin, carcinogenesis and skin metabolism[5], no special attention has been paid to their immune disorders until our previous reports pointed out that homozygous rhino mice had a systemic connective tissue

Fig. 13. Electron micrograph of fibrotic area of liver of rhino mouse showing appearance of collagen fibers (CF), plasma cells (P) and a plasmablast (Pb) adjacent to the hepatic cells (HC). Electron-dense deposits are present among collagen fibers which are transversely or longitudinally sectioned. The insert shows microfibrillar structures of dense deposits and electron-lucent transverse sections of collagen fibers. × 5200, insert × 39,000.

Fig. 14. Electron micrograph of renal glomerulus showing irregular thickening of capillary basement membrane (BM) and electron-dense deposits (arrows). Fusion of epithelial foot processes (FP) are noted. End, Endothelial cell; Ep, Epithelial cell; Mes, Mesangial cell; CL, Capillary lumen. × 1300.

disease associated with lymphoreticular abnormalities and spontaneous hypergammaglobulinemia[15,16].

The present study demonstrated that ANA, one of the adequate markers of possible autoimmune disease, was detectable by indirect IF in the sera of homozygous rhino mice with very high frequency and nearly 100% of homozygous rhino mice aged over 5 months developed ANAs with very high titers. Albeit moderately enhanced incidence of ANA was also observed in mice having heterozygous rhino gene, no prominent increase in titers of ANA and no gross evidence of accompanying disease could be detected in these heterozygous mice. Accordingly, it is suggested that homozygousness for rhino gene plays an essential role in the manifestations of systemic connective tissue disease associated with occurrence of ANA. ANA, as detected by IF in NZB mice has been reported to occur at a low incidence (less than 5%) during the first few weeks of age and not more than 15–45% of the mice developed ANA even at old ages[11,23]. SIEGEL *et al.*[30] have reported that 90% of 5-week-old NZB mice were found to develop ANA detectable by the use of formalinized nuclei isolated from chicken erythrocytes. SIEGEL's experiment and our present observation suggest that the chicken erythrocyte nuclei provide a sensitive and suitable assay system for the detection of ANA.

Although ANA has also been reported to occur spontaneously in certain strains of mice, such as A/J, C57BL, CBA, C3H, DBA/2, AKR, BALB/c, SJL, 129/J and HI[2,7,30], these ANAs have been found to develop only at low incidence and at low titer. However, these strains of mice, unlike New Zealand mice did not develop gross and histological evidence accompanying lupus-like lesions.

The nephritis in New Zealand mice and human lupus patients has been found to correlate closely with the glomerular deposition of immune complex and complement. IF and elution have indicated that nuclear antigens including DNA and their antibodies were concentrated in the renal deposits implicating this particular immune complex in the pathogenesis of nephritis[17,18].

ANA has also been detected in areas of skin actively involved with SLE rash. These deposits, found at the dermal-epidermal junction, also contained bound complement[26]. Recently, immunoglobulin deposits have been found at the dermal-epidermal junction of clinically uninvolved skin of patients with SLE[8] as well as of New Zealand mice[9], and the occurrence of these deposits have been correlated with the presence of immune complex in the kidney.

The characteristic hyperkeratosis and cyst formation are spontaneously found in the skin of rhino mice and these phenomena are controlled by homozygous rhino gene. During the process of rapid keratinization, epidermal nuclei are broken down and nuclear materials including DNA may be liberated. Recently, it was reported that DNA can be actively bound *in vitro* by collagen or glomerular basement membrane and DNA thus bound can act as immunoabsorbant and react efficiently with free anti-DNA antibodies[14]. It is possible that nuclear antigens including DNA released from epidermal cells would bind to the basement membrane of dermal-epidermal junction and collagen of subepidermal connective tissue of skin of rhino mice. This may be the

reason why the earliest site of IgG deposition in rhino mice is the skin.

Additional lesion reported in New Zealand mice is chronic active hepatitis reminiscent of human lupoid hepatitis with peculiar splenic fibrosis[6,23]. Accordingly, the renal, hepatic, splenic and skin lesions of rhino mice have a close similarity to those seen in New Zealand mice[6,10,18,23] and human SLE[17,26,30]. Among these lesions, hepatic fibrosis accompanied by plasma cell infiltration seems to be the most prominent feature in rhino mice. Hepatic lesions resembling those seen in rhino mice have been noted by PAGE and GOOD[25] in patients with plasma cell hepatitis which was characterized clinically and pathologically by extreme hypergammaglobulinemia and by plasma cell infiltration along the parenchyma of liver, respectively. Cortisone therapy in this group of patients produced dramatic suppression of the liver disease.

Although the etiology and pathogenesis of the hepatic lesions of rhino mice are not fully elucidated at present, the failures to detect antibodies against MHV and coronavirus-like particles by electron microscopy suggested that MHV infection is not related to these hepatic lesions.

Further, electron microscopic studies revealed that irregular masses of electron-dense deposits were present within and on both sides of the thickened capillary basement membrane of renal glomerulus, among the collagen fibers of fibrotic areas of liver and at the dermal-epidermal junction as well as among the collagen fibers of dermis of rhino mice. The sites of these deposits corresponded to those of deposition of IgG and C3, as shown by IF. The series of these changes were analogous to those seen in NZB mice[4,18,22,23,32] and patients with SLE[10,29], but organized structures[10] of dense deposits were not found in rhino mice.

The deposition of IgG in the corneal stroma, and degeneration of collagen fibers associated with their irregular arrangement have been seen in the eye of rhino mice[1]. Our present observations on the eye confirmed these findings.

In addition to nuclear antigens, another antigen deposited in the form of Ag-Ab complex was found to be murine leukemia virus (MLV) antigen in New Zealand mice[23, 32]. Although the present electron microscopic observation indicated that C-type virus-like particles were not detected so far in the lesions of skins, livers and kidneys of rhino mice, further studies on the distribution of virus specific protein antigens of retro-virus, such as gp 70 and p 30, may elucidate the nature of immune complex in rhino mice[13].

In order to characterize the immunological properties of tissue-bound globulin, elution study was undertaken from the tissue of livers, kidneys, skins, spleens and lumph nodes of rhino mice aged between 7.5 and 18 months. By use of immuno-electrophoretic and IF techniques, acid eluates from livers and kidneys were found to contain IgG with ANA activity. Accordingly, it is conceivable that at least a part of tissue-bound gloublins is identical with ANA and that the immunoglobulins are deposited in the form of Ag-Ab complex.

Recent work in our laboratory demonstrated that rhino mice were found to show a progressive depletion of thy-1 positive lymphocytes (T-cell) and gradual increase in the population of surface Ig-bearing lymphocytes (B-cell) in lymphoid organs during

aging. Depressed immune responses against allogenic tumor transplantation and thymus dependent antigens, such as sheep erythrocytes and bovine serum ablumin was also noted in old age of these mice[15,16]. Histological examinations revealed that early involution of thymus associated with depletion of cortical lymphocytes, marked decrease of small lymphocytes in the thymus-dependent area of lymph nodes and spleen and prominent proliferation of plasma cells in almost all the lymphoid organs were consistently observed in rhino mice with increasing age[15,16]. From the view point of functional activity and morphological structure of lymphoid organs, rhino mice are in the state of T-cell deficiency and B-cell stimulation like New Zealand mice[31,32]. This suggests that diminished T-cell activity and excessive B-cell activity may favor the appearance of autoimmunity. More recently, decline of suppressor T-cell function was reported in aged NZB mice and this phenomenon was assumed to be related to autoantibody production[3].

Certain common characteristics of "markers" of autoimmune disease have been described by MACKAY and BURNET[20]. These include hypergammaglobulinemia; the demonstration of autoantibodies against a body component; immunoglobulin deposition in the affected tissue, such as renal glomerulus; the accumulation of lymphocytes and plasma cells in the tissue damaged by autoimmune processes; and multiple autoimmune manifestations in the same individual. Our present and previous observations revealed that the adult rhino mice possess all of these characteristics. Consequently, rhino mice might be considered to be a desirable experimental model of a genetically controlled multi-systemic autoimmune disease. Further studies of these mice, which are in progress in our laboratory, will provide valuable information concerning pathogenesis, etiologic factors and abnormal immune status in autoimmune diseases.

Acknowledgements: The authors are grateful to Prof. M. HANAOKA, Dept. Pathology, Institute for Virus Research, Kyoto University, Prof. Y. HAMASHIMA and Dr. S. IKEHARA, Dept. Pathology Faculty of Medicine, Kyoto University and Dr. T. Masuda, Institute for Immunology, Kyoto University for their valuable comments on the manuscript. The authors also thank Dr. Z. SUZUOKI and Dr. Y. SUGINO for their helpful advice and encouragment during the course of this study. The excellent technical assistance of Messrs. K. MIYAMOTO, K. HIKAWA, T. GOTO, and E. IBA is appreciated.

References

1. AMEMIYA, T., YOSHIDA, H., YOSHIDA, M., and KAWAJI, H.: Ocular pathology of rhino mouse. I. Ultrastructure of the cornea – A model of corneal dystrophy. Acta Soc. Ophthalm. Jap. **81**: 1814–1821, 1977 (*in Japanese*).
2. BARNES, R.D. and TUFFREY, M.: Serum antinuclear factor and influence of environment in mice. Nature **214**: 1136–1138, 1967.
3. BARTHOLD, D.R., KYSELA, S., and STEINBERG, A.D.: Decline in suppressor T cell function with age in female NZB mice. J. Immunol. **112**: 9–16, 1974.
4. CHANNING, A.A., KASUGA, T., HOROWITZ, R.E., DUBOIS, E.L., and DEMEPOULS, H.B.: An ultrastructural study of spontaneous lupus nephritis in the NZB/BL-NZW mouse. Am. J. Path. **47**: 677–694, 1965.
5. DAVIES, R.E., AUSTIN, W.A., and LOGANA M.K.: The rhino mutant mouse as an experimental tool. Transact. N.Y. Acad. Sci. Series II **33**: 680–693, 1971.

6. DUBOIS, E.L., HOROWITZ, R.E., DEMEPOULOS, H.B., and TEPLITZ, R.: NZB/NZW mice as a model of systemic lupus erythematosus. J. Amer. Med. Ass. **195**: 285–289, 1966.
7. FRIOU, G.J. and TEAGUE, P.O.: Spontaneous autoimmunity in mice: Antibodies to nucleoprotein in strain A/J. Science **143**: 1333–1334, 1964.
8. GILLIAM, J.N., CHEATUM, D.E., HURD, E.R., STASTNY, P., and ZIFF, M.: Immunoglobulin in clinically uninvolved skin in systemic lupus erythematosus. J. Clin. Invest. **53**: 1434–1440, 1974.
9. GILLIAM, J.N., HURD, E.R., and ZIFF, M.: Subepidermal deposition of immunoglobulin in NZB/NZW F1 hybrid mice. J. Immunol. **114**: 133–137, 1975.
10. GRISHMAN, E., and CHURG, J.: Ultrastructure of dermal lesions in systemic lupus erythematosus. Lab. Invest. **22**: 189–197, 1970.
11. HAHN, B.H. and SHULMAN, L.: Autoantibodies and nephritis in the white strain (NZW) of New Zealand mice. Arthritis Rheum. **12**: 355–364, 1969.
12. HOWARD, A.: "Rhino" an allele of hairless in the house mouse. J. Heredity **31**: 467–470, 1940.
13. IMAMURA, M., MELLORS, R.C., STRAND, M., and AUGUST, J.T. Murine type C viral envelop glycoprotein gp 69/71 and lupus-like glomerulonephritis of New Zealand mice. Am. J. Path. **86**: 375–381, 1977.
14. IZUI, S., LAMBERT, P.H., and MIESCHER, P.A.: In vitro demonstration of a particular affinity of glomerular basement membrane and collagen for DNA. A possible basis for a local formation of DNA-anti-DNA complexes in systemic lupus erythematosus. J. Exp. Med. **144**: 428–443, 1976.
15. KAWAJI, H.: Abnormality of lymphoreticular tissue observed in rhino mouse. Acta Haem. Jap. **30**: 93–103, 1963 (*in Japanese*).
16. KAWAJI, H.: Sutiability of rhino mouse in studies of connective tissue disease. Exp. Animals **22**, Supple.: 299–310, 1973.
17. KOFFLER, D., SCHUR, P.H., and KUNKEL, H.G.: Immunological studies concerning the nephritis of systemic lupus erythematosus. J. Exp. Med. **126**: 607–631, 1967.
18. LAMBERT, P.H., and DIXON, F.: Pathogenesis of the glomerulonephritis of NZB/W mice. J. Exp. Med. **127**: 507–513, 1968.
19. LEWIS, R.M.: Spontaneous autoimmune disease of domestic animals. Internat. Rev. Exp. Path. **13**: 55–160, 1971.
20. MACKAY, I.R. and BURNET, F.M.: in KUGELMASS, I.N. (Ed.), The Autoimmune Diseases: Definition and general character of autoimmune disease, 14–21. Charles C. Thomas, Springfield, Illinois, 1963.
21. MANCINI, G., CARBONARA, A.O., and HEREMANS, J.F.: Immunochemical quantitation of antigens by single radial immunodiffusion. Immunochem. **2**: 235–254, 1965.
22. MCGIVEN, A.R., and Lynraven, G.S.: Glomerular lesions in NZB/NZW mice. Electron microscopic study of development. Arch. Path. **85**: 250–261, 1968.
23. MELLORS, R.C.: Autoimmune and immunoproliferative disease of NZB/BL mice and hybrids. Internat. Rev. Expt. Pathol. **5**: 217–252, 1966.
24. MORSE, H.C., STEINBERG, A.D., SCHUR, P.H., and REED, N.D.: Spontaneous "autoimmune disease" in nude mice. J. Immunol. **113**: 688–697, 1974.
25. PAGE, A.R. and GOOD, R.A.: Plasma cell hepatitis. Lab. Invest. **11**: 351–359, 1962.
26. PELTIER, A.P. and ESTES, D.: in HARRY, L.I. (Ed.), Pathobiology Annual: Antinuclear antibodies, Vol 2, 77–109. Appleton-Century Crofts, New York, 1972.
27. PELLETIER, M., HINGLAIS, N., and BACH, J.: Characteristic immunohistochemical and ultrastructural glomerular lesions in nude mice. Lab. Invest. **32**: 388–396, 1975.
28. SAINTE-MARIE, G.: A paraffin embedding technique for studies employing immunofluorescence. J. Histochem. **10**: 250–256, 1962.
29. SCHREINER, E. and WOLF, K.: Systemic lupus erythematosus: Electron microscopic localization of in vivo found gloublin at the dermal-epidermal junction. J. Invest. Dermatol. **55**: 325–328, 1970.
30. SIEGEL, B.V., BROWN, M., and MORON, J.I.: Detection of antinuclear antibodies in NZB and other mouse strains. Immunology **22**: 457–463, 1972.
31. STUTMAN, O.: Lymphocyte subpopulations in NZB mice: Deficit of thymus-dependent lymphocytes. J. Immunol. **109**: 602–611; 1972.

32. TALAL, N. and STEINBERG, A.D.: The pathogenesis of autoimmunity in New Zealand Black mice. Current Topics in Microbiology and Immunology **64**: 79–103, 1974.
33. TEN VEEN, J.H., and FELTKAMP, T.E.W.: Formalinized checken red cell nuclei as a simple antigen for standardized antinuclear factor determination. Clin. Exp. Immunol. **5**: 673–678, 1969.
34. WILLIAMS, C.A.: in WILLIAMS, C.A. and CHASE, M.W. (Eds.), The Methods in immunology and immunochemistry: Immunoelectrophoretic analysis in agar gels, Vol. III, 237–273. Academic Press, New York and London, 1971.